



Article

Extraction of Polyphenols and Vitamins Using Biodegradable TPS Based on Ethyl Lactate

Pedro Velho ^{1,2} , Luís Marques ^{1,2} and Eugénia . Macedo ^{1,2,*} 

¹ LSRE-LCM—Laboratory of Separation and Reaction Engineering—Laboratory of Catalysis and Materials, Faculty of Engineering, University of Porto, Rua Dr. Roberto Frias, 4200-465 Porto, Portugal

² ALiCE—Associate Laboratory in Chemical Engineering, Faculty of Engineering, University of Porto, Rua Dr. Roberto Frias, 4200-465 Porto, Portugal

* Correspondence: eamacedo@fe.up.pt; Tel.: +351-220-411-653

Abstract: The growing human population, together with the inefficient use of natural resources, has been dramatically increasing the production of food waste, which poses serious economic, environmental, and social problems. Being so, it is necessary to increase the efficiency of food consumption so as to reduce its waste and to convert the remaining residues into societal benefits. Since this biowaste is rich in polyphenols and vitamins, it could become the feedstock for the production of important value-added compounds for the pharmaceutical (*e.g.*, food supplements) and cosmetic (*e.g.*, creams and shampoos) industries. In this work, partition studies of one polyphenol (epicatechin) and two B-complex vitamins (cyanocobalamin and nicotinic acid) were performed in biodegradable Aqueous Two-Phase Systems (ATPS) based on ethyl lactate and on organic salts (disodium tartrate, tripotassium citrate, and trisodium citrate) at 298.15 K and 0.1 MPa. The largest partition coefficient (*K*) and extraction efficiency (*E*) were obtained for vitamin B12 (*K* = 78.56, *E* = 97.5%) for the longest tie line (TLL = 77.66%) in the ATPS {ethyl lactate (1) + tripotassium citrate (2) + water (3)}. All the extractions were obtained with low biomolecule mass losses in quantification (<5%) and after a thorough study of pH influence in the UV–Vis absorbance spectra.

Keywords: ATPS; ethyl lactate; polyphenols; vitamins



Citation: Velho, P.; Marques, L.; Macedo, E.A. Extraction of Polyphenols and Vitamins Using Biodegradable ATPS Based on Ethyl Lactate. *Molecules* **2022**, *27*, 7838. <https://doi.org/10.3390/molecules27227838>

Academic Editors: Francesco Cacciola and Katia Arena

Received: 26 September 2022

Accepted: 11 November 2022

Published: 14 November 2022

Publisher's Note: MDPI stays neutral with regard to jurisdictional claims in published maps and institutional affiliations.



Copyright: © 2022 by the authors. Licensee MDPI, Basel, Switzerland. This article is an open access article distributed under the terms and conditions of the Creative Commons Attribution (CC BY) license (<https://creativecommons.org/licenses/by/4.0/>).

1. Introduction

The steady growth of the human population, together with the inefficient use of natural resources, has been contributing to an increased production of food waste, which poses serious economic and social problems [1,2]. Furthermore, environmental issues such as farm-level water losses, land degradation, and greenhouse gas emissions from food distribution and decomposition are also linked to this global problem [2]. Being so, it is necessary to increase the efficiency of food consumption and to convert the remainder of this waste into societal benefits.

Successful attempts of using food waste as feedstock and contributing to a more circular economy are common in the literature, including its application in the production of fertiliser [3,4] and of insects for human food and animal feed [4]. Moreover, a particular type of sustainable biorefinery, the food waste biorefinery, has been gaining preponderance as a source of added-value compounds [5] and as a processual precursor of waste incineration and fertiliser production. This way, important biomolecules such as enzymes, peptides, fatty acids (*e.g.*, from fish processing wastes [5]), glucose, collagen, keratin (*e.g.*, from meat processing wastes [5]), vitamins, and polyphenols (*e.g.*, from fruit peels and pomaces [6,7]) are recovered and applied in the pharmaceutical and cosmetic industries and even reintroduced in the food sector [7,8].

Aqueous Two-Phase Systems (ATPS) or Aqueous Biphasic Systems (ABS) have emerged as a powerful tool for the recovery of biomolecules, for the analysis of cellular surfaces, and for the fractionation of cell populations [9]. Generally, ATPS are composed by a ternary

mixture of water + polymers, water + polymer + salt, or water + organic solvent + salt. The presence of a salting-out agent (*e.g.*, salt or polymer) induces phase splitting and yields two liquid phases, known as top (lower density) and bottom (higher density) phases, with one of them being significantly richer in salting-out agent than the other. The distinct phase compositions create differences in properties such as hydrophobicity, polarity, and viscosity, which will rule solute migration (partition) between the phases. Since both their liquid phases are mostly composed by water, ATPS are gentle and biocompatible media for biomaterials and are characterised by low interfacial tensions when compared, for example, with conventional water/organic solvent systems [9,10].

Polyethylene glycol (PEG) is the most applied polymer for its nontoxicity, relative low-cost, and ease of synthesis [11], but product recovery is extremely hard and requires the handling of less eco-friendly solvents. PEG has been applied in the extraction of, for example, amino acids [12,13], active pharmaceutical ingredients (API) [14], flavonoids [15], and proteins [16].

Ethyl lactate is an environmentally benign bio-based green solvent with large solvating power. It is a hydrophilic, amphiphilic, bio-renewable, non-flammable, and biodegradable chemical with growing application as sustainable media for organic synthesis [17,18]. Further, it is also being used as a food additive, paint stripper, flavour chemical, and in perfumery [19,20]. Recently, ethyl lactate has been applied to extract biomolecules such as vitamins [21,22], pigments [22,23], antioxidants [24–26], amino acids [27], proteins [28], and antibiotics [29], replacing more hazardous solvents such as alcohols and dichloromethane.

Concerning salts, inorganic salts such as sulphates [30,31] and phosphates [30,32] have been extensively used in ATPS, but these may cause environmental distress at an industrial scale of operation [11]. Therefore, organic salts such as tartrates [12,30] and citrates [13,30] have been preferred due to their non-toxicity and biodegradability.

Recently, some novel ATPS have been developed to enforce the recyclability of their constituents and the selectivity for certain species, such as ATPS based on light-triggered switchable ionic liquids [33], on choline amino acid ionic liquids [34], and on surfactants and polyalcohols [35].

In this work, three biomolecules were studied, including one polyphenol (epicatechin) and two B-complex vitamins (cyanocobalamin and nicotinic acid).

Epicatechin (E) belongs to a particular category of polyphenols, the flavonoids, which are products of the secondary metabolism of plants [36]. Epicatechin is commonly found in a wide variety of foods, such as fruits (*e.g.*, apples, grapes, cherries, and apricots), vegetables, legumes, cocoa derivatives, wine, and some teas [37,38]. This catechin has been shown to reduce hypertension, to improve the endothelial function [39], and is thought to enhance cognition [40].

Cyanocobalamin or vitamin B12 is a corrinoid which can be found in red meat, milk, eggs, potatoes, and mushrooms [41]. It is essential for the normal functioning of the human body, especially to what concerns methylation and the mitochondrial metabolism, so its severe deficiency has been found to cause haematological (*e.g.*, megaloblastic anaemia) and neurological (*e.g.*, demyelination of the peripheral and central neurons) issues [42].

Nicotinic acid (NA) is one of the forms of vitamin B3. It is a water-soluble vitamin and has been extensively used as a lipid-modifying drug due to its antidiyslipidemic properties (counteracts the imbalance of lipids in blood) [43]. Significant quantities of nicotinic acid have been found in legumes and fruits, with chestnuts, figs, melons, peaches, and cherries being some of the most relevant [44]. Figure 1 summarizes the natural sources of the studied biomolecules in this work.

The aim of this work was to delve into the extraction of one polyphenol (epicatechin) and two vitamins (cyanocobalamin and nicotinic acid) so as to set the ground for future valorisation of food wastes (*e.g.*, vegetable peels and fruit pomaces) to value-added pharmaceutical (*e.g.*, food supplements) and cosmetic (*e.g.*, creams and shampoos) products. Different biodegradable and ethyl-lactate-based ATPS with organic salts were applied at 298.15 K and 0.1 MPa in the partition of these biomolecules for the first time, in an effort

to find effective extraction media which could promote a more sustainable production of therapeutics and cosmetics and a more circular economy.

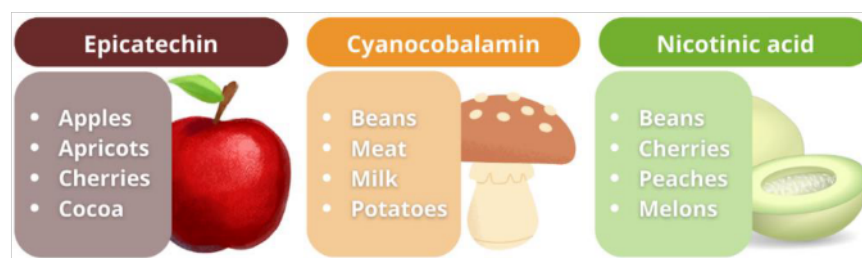


Figure 1. Possible feedstocks for the extraction of epicatechin [37,38], cyanocobalamin (vitamin B12) [41], and nicotinic acid [44].

2. Materials and Methods

2.1. Chemicals

Table 1 presents the chemicals used in this work, together with their respective commercial suppliers, purities, Chemical Abstracts Service (CAS) number, and abbreviation. All the chemicals were used without any further purification step.

Table 1. Chemicals used in this work, with respective chemical formula, suppliers, purities, CAS number, and abbreviation.

Chemical	Supplier	Purity ^a /m% ^b	C S	bbreviation
Acetic acid (CH ₃ COOH)	Merck	>99.8	64-19-7	-
Cyanocobalamin or vitamin B12 (C ₆₃ H ₈₈ CoN ₁₄ O ₁₄ P)	Sigma-Aldrich	>98	68-19-9	B12
(-)-epicatechin (C ₁₅ H ₁₄ O ₆)	Tokyo Chemical Industry	>97	490-46-0	E
Ethanol (CH ₃ CH ₂ OH)	Sigma-Aldrich	>99	64-17-5	-
(-)-ethyl L-lactate (C ₅ H ₁₀ O ₃)	Sigma-Aldrich	>98	97-64-3	EL
Nicotinic acid (C ₆ H ₅ NO ₂)	Sigma-Aldrich	>99.5	59-67-6	NA
Purified water (H ₂ O)	VWR chemicals	-	7732-18-5	W
Sodium hydroxide (NaOH)	Merck	>99	1310-73-2	-
Potassium citrate monohydrate (C ₆ H ₅ K ₃ O ₇ ·H ₂ O)	Sigma-Aldrich	>99	6100-05-6	K ₃ Citrate
Sodium citrate tribasic dihydrate (C ₆ H ₅ Na ₃ O ₇ ·2H ₂ O)	Sigma-Aldrich	>99	6132-04-3	Na ₃ Citrate
Sodium tartrate dihydrate (C ₄ H ₄ Na ₂ O ₆ ·2H ₂ O)	VWR chemicals	>99.9	6106-24-7	Na ₂ Tartrate

^a Provided by the supplier; ^b m% refers to mass percentage.

2.2. Apparatus and Experimental Procedure

In this work, an ADAM AAA 250L balance with measurement uncertainty of $\pm 10^{-4}$ g was used to assess mass (m), and a Thermo Scientific Varioskan Flash spectrophotometer with measurement uncertainty of $\pm 10^{-4}$ was used to determine UV–Vis absorbance (A). Further, temperature (T) was kept at 298.15 ± 0.01 K with a Julabo F12 thermostatic bath coupled with a Julabo ED controller, and density (ρ) was assessed using an Anton Paar DSA-5000M densimeter with measurement uncertainties of $\pm 3 \times 10^{-5}$ g·cm^{−3} in density and ± 0.01 K in temperature. Lastly, pH was evaluated using a VWR pH1100L with measurement uncertainties of ± 0.001 in pH and ± 0.1 K in temperature.

2.2.1. Influence of System's pH in the UV–Vis Absorbance Spectra

To assess the influence of the phases' pH in the UV–Vis absorbance spectra of the biomolecules, aqueous stock solutions with different pH values and with concentrations of about $(1.54, 3.12, \text{ and } 2.50) \times 10^{-4}$ g·mL^{−1} were prepared for epicatechin, cyanocobalamin, and nicotinic acid, respectively. In the determinations, the maximum concentrations were defined by the solubility in water of the species and by the useful absorbance range of the spectrophotometer. The pH values of the solutions were adjusted by adding droplets of 0.5 M sodium hydroxide (NaOH) or 0.5 M acetic acid (CH₃COOH) aqueous solutions. Afterwards, 200 μ L samples of each solution were added to a Greiner bio-one polystyrene flat bottom plate, and an absorbance scanning was performed from 200 to 600 nm using the Thermo Scientific Varioskan Flash UV–Vis spectrophotometer, after having stabilised the samples at 298.15 K.

Moreover, to evaluate the stability of the UV–Vis absorbance spectra at different pH values, the solutions were left to settle for 3 days at 298.15 K without any especial protection from daylight, after which a new absorbance screening was conducted with the UV–Vis spectrophotometer following the same procedure. These two spectra were then compared to evaluate the stability of the UV–Vis spectra at the different pH values.

2.2.2. UV–Vis Absorbance Calibration Curves

To determine adequate UV–Vis absorbance calibration curves, 2 mL aqueous mixtures with different concentrations of biomolecule (epicatechin, cyanocobalamin, or nicotinic acid) were prepared in vials by diluting fresh stock solutions at a pH value of ~ 7.5 , which was considered close to the characteristic pH of all the different ATPS used. After being capped and sealed with parafilm, the vials were vigorously stirred in a VWR VV3 vortex for about 2 min and in an IKA RO 10 P magnetic stirrer for 20 min. Afterwards, 200 μ L samples of each vial were taken to the Thermo Scientific Varioskan Flash UV–Vis spectrophotometer, and an absorbance scanning, from 200 to 600 nm, was performed following the previously explained procedure. Then, the UV–Vis calibration curves were determined by plotting the biomolecules' concentrations with the absorbances at a chosen wavelength and fitting the data to a first-degree equation after having subtracted the absorbance of blanks. The chosen wavelengths were 278, 363, and 264 nm for epicatechin, cyanocobalamin, and nicotinic acid, respectively. The absorbance of eventual pH adjusters (NaOH or CH₃COOH) was considered negligible.

2.2.3. Liquid–Liquid Extraction of Biomolecules

Vials with mixtures of 10 mL were prepared corresponding to the known tie lines (isothermal lines which connect two corresponding phases) of the ATPS {ethyl lactate (1) + disodium tartrate (2) + water (3)} [24], {ethyl lactate (1) + trisodium citrate (2) + water (3)} [25], and {ethyl lactate (1) + tripotassium citrate (2) + water (3)} [25], which were determined in previous works of the research group. These mixtures were prepared by pipetting and weighing the pure compounds (water and ethyl lactate) and the aqueous solutions of the organic salts: disodium tartrate (30.00 m%), trisodium citrate (25.59 m%), and tripotassium citrate (32.75 m%). In the preparation of the mixtures, 1 mL of the reported water content in [24,25] was replaced by 1 mL of stock solution of the biomolecule being

studied (epicatechin, cyanocobalamin, or nicotinic acid). After being stirred in a vortex for 2 min, the samples were left under stirring for 6 h in the Julabo F12 thermostatic bath at 298.15 K. Then, the vials were left settling overnight (~12 h) at the same temperature. Afterwards, the top and bottom phases were carefully removed using pipettes and weighed in the ADAM AAA 250L balance. Moreover, the UV–Vis absorbances, the pH values, and the densities of the two phases of each tie line were assessed, by this order, with the Thermo Scientific Varioskan Flash spectrophotometer, VWR pH 1100 L pH meter, and Anton Paar DSA-5000M densimeter, respectively. The densimeter was cleaned between measurements with water and ethanol.

3. Results and Discussion

Due to the lability of vitamins and antioxidant species (such as polyphenols), their chemical formula/conformation can be changed by the pH of the liquid phase, causing the appearance of new chemical compounds. The differently charged species that a biomolecule may present, also known as stages [21], generally show different affinities to the ATPS phases, so properly identifying the stages which are present in a solution is essential to study biomolecule-oriented extractive processes.

Since the decimal logarithms of the dissociation constants (pK_a) of epicatechin (8.72, 9.49, 11.23, and 13.40 [45]), cyanocobalamin (3.28 [46]), and nicotinic acid (2.00 and 4.82 [47]) are available in literature, the ratios between two successive biomolecule stages, *i.e.*, between a biomolecule of a certain charge and its closest reduced state, can be determined as a function of pH using Equation (1) [21]:

$$\frac{[S^{q_0-i-1}]}{[S^{q_0-i}]} = 10^{pH_{\text{phase}} - pK_a^i} \quad (1)$$

where q_0 is the charge of the antioxidant at $pH = 0$, i is the number of the dissociation constant (pK_a^i) being considered, pH_{phase} is the pH of the phase under study, and $[S^{q_0-i-1}]$ and $[S^{q_0-i}]$ are the molar concentrations of the biomolecule stages with electrical charges of $(q_0 - i - 1)e$ and $(q_0 - i)e$, respectively. e stands for the elementary charge ($1.602 \cdot 10^{-19}$ C).

Then, the mean electrical charge of the antioxidant (q) can be calculated using a weighted arithmetic mean:

$$q = \sum_{i=1}^{i_{\max}} \left[x_{S^{q_0-i-1}} \times (q_0 - i - 1) \right] \quad (2)$$

where $x_{S^{q_0-i-1}}$ is the fraction (relative abundance) of the biomolecule stage with an electrical charge equal to $(q_0 - i - 1)e$.

In Figure 2, the calculated mean electrical charges (q) at different pH values for the studied biomolecules (epicatechin, cyanocobalamin, and nicotinic acid) can be seen.

In this work, the partition studies of epicatechin, cyanocobalamin, and nicotinic acid were performed in the ATPS shown in Table 2. According to the available literature [24,25], the phase separation of these ATPS causes pH values from 6 to 8. As observed in Figure 2, in this range, the mean electrical charges (q) of these biomolecules correspond almost entirely to an integer value, so only one species (stage) is present, which allows better characterisation of the final extract. In Tables S1–S3 in the Supplementary Materials, the fractions of each biomolecule stage (x_S) for the data shown in Figure 2 can be observed. There, it can be noticed that, for example, at $pH = 7.5$, the molar fractions of the most common stages of epicatechin (E), cyanocobalamin (B12), and nicotinic acid (NA) are, respectively, $x_{E^0} = 0.94$, $x_{B12^{-1}} = 1.00$, and $x_{NA^{-2}} = 1.00$.

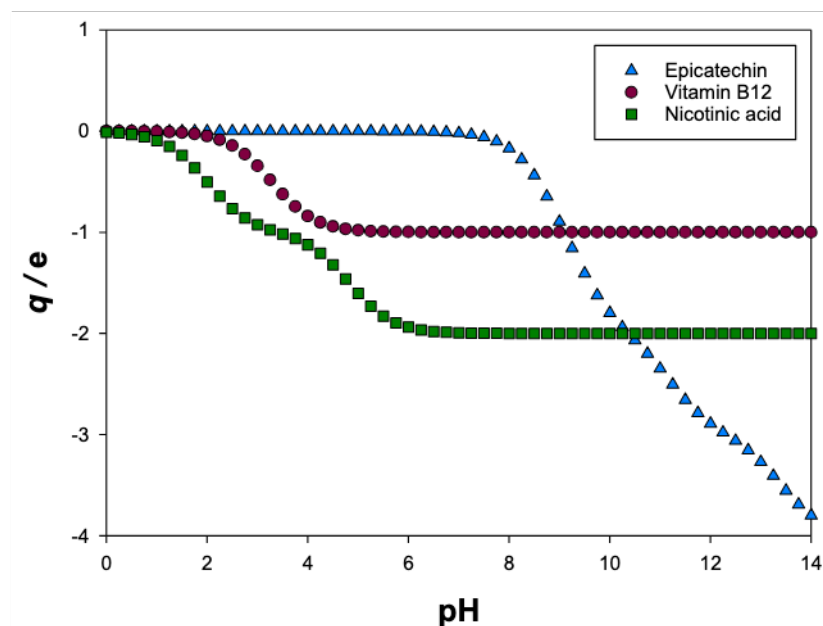


Figure 2. Calculated mean electrical charge (q) for epicatechin, cyanocobalamin (vitamin B12), and nicotinic acid, expressed in terms of the elementary charge (e), i.e., 1.602×10^{-19} C.

Table 2. Extracted biomolecules using the Aqueous Two-Phase Systems (ATPS) {ethyl lactate (1) + organic salt (2) + water (3)}.

Biomolecule	Organic Salts		
	Na ₂ Tartrate	Na ₃ Citrate	K ₃ Citrate
Epicatechin	×		×
Cyanocobalamin	×		×
Nicotinic acid	×	×	

3.1. Influence of pH in the UV–Vis Absorbance Spectra

As previously stated, the relative abundance of each biomolecule stage is heavily influenced by pH, since its variation leads to changes in the chemical structure and/or chemical conformation. Being so, the UV–Vis absorbance spectrum may also be altered, for which studying the influence of pH will be crucial for accurately determining the calibration curves. Therefore, absorbance measurements were performed from 200 to 600 nm in aqueous solutions with different pH values and with concentrations of about $(1.54, 3.12, \text{ and } 2.50) \times 10^{-4} \text{ g} \cdot \text{mL}^{-1}$ for epicatechin (Figure 3), cyanocobalamin (Figure S1), and nicotinic acid (Figure S2), respectively. These absorbance spectra were normalised, having in consideration the amount of pH adjusters (0.5 M NaOH and 0.5 M CH₃COOH) added using Equation (3), so as to ease interpretation.

$$I = \frac{C_{\text{pH}=7.5}}{C_{\text{pH}=k}} \quad (3)$$

Here, I is the experimental UV–Vis absorbance for a given wavelength (λ), I' is the normalised absorbance, $C_{\text{pH}=7.5}$ is the reference concentration (pH = 7.5), and $C_{\text{pH}=k}$ is the concentration of the stock solution of biomolecule at a given pH k .

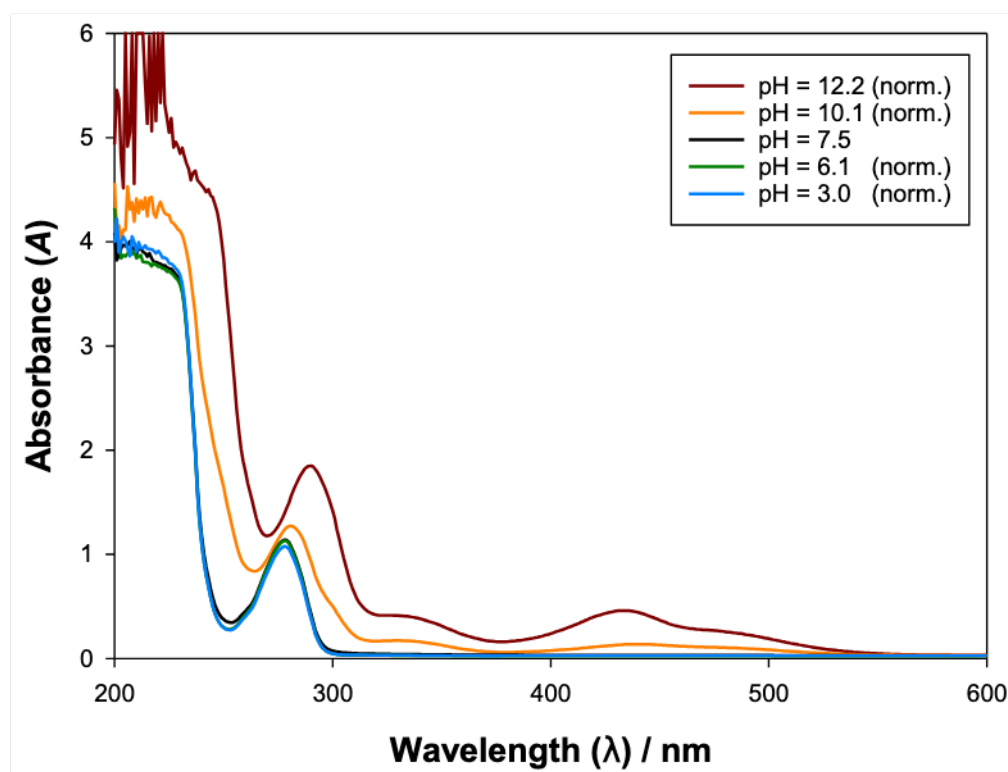


Figure 3. Influence of pH in the UV–Vis absorbance spectra of epicatechin ($3.12 \times 10^{-4} \text{ g}\cdot\text{mL}^{-1}$) at 298.15 K and 0.1 MPa.

As Figure 3 shows for epicatechin, larger pH values imply larger UV–Vis absorbances and a progressively higher wavelength for the local maximum verified at 278 nm (and pH = 7.5). For cyanocobalamin (Figure S1) and nicotinic acid (Figure S2), the found spectra were almost independent of pH, hinting remarkably similar absorbance for all their biomolecule stages, which generally ensures more precise quantification of their concentrations using UV–Vis absorbance calibration curves.

3.2. UV–Vis Absorbance Calibration Curves

To enable an adequate quantification of the biomolecules after phase separation, UV–Vis calibration curves were determined at the wavelengths of 278, 363, and 264 nm for epicatechin, cyanocobalamin, and nicotinic acid, respectively. The UV–Vis absorbance spectra of the studied biomolecules can be seen in Figure 4. The calibration curves were conducted at a pH value close to the ones available in the literature for the studied ATPS (pH \approx 7.5) and can be observed in Figure 5. In the determinations, the absorbance of water (and plate) was subtracted, and the calibration curves were determined at the wavelengths that corresponded to the local or global maxima in which the other ATPS species (ethyl lactate and organic salts) and pH adjusters (NaOH and CH_3COOH) did not significantly interfere.

Furthermore, since partition determinations take around 18 h (6 h of stirring and 12 h of settling), it is essential for the UV–Vis absorbance spectra to remain constant so as to be able to apply the found calibration curves (Figure 5). Being so, the prepared aqueous solutions of the studied biomolecules were left settling for three days without any especial protection from daylight, and their absorbance spectra were measured and compared to the initial ones. As Figures S3–S5 in the Supplementary Materials show, the chosen absorbance maxima were not affected by 3 days of settling, so their usage after \sim 18 h was validated.

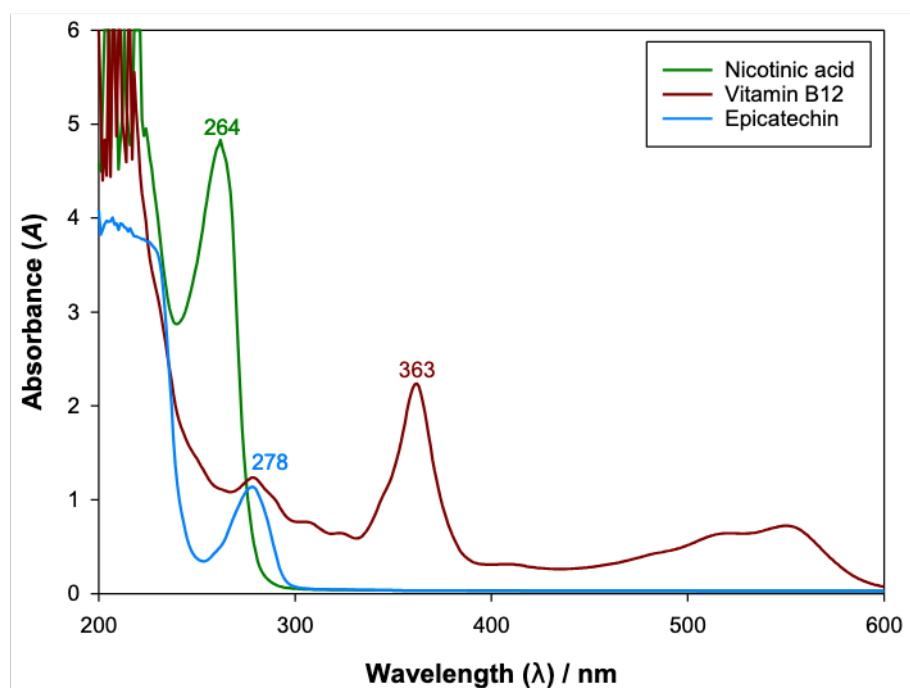


Figure 4. UV-Vis absorbance spectra at pH = 7.5, from 200 to 600 nm, for epicatechin, cyanocobalamin (vitamin B12), and nicotinic acid at $(1.54, 3.12, \text{ and } 2.50) \times 10^{-4} \text{ g}\cdot\text{mL}^{-1}$, respectively, with $T = 298.15 \text{ K}$ and $P = 0.1 \text{ MPa}$.

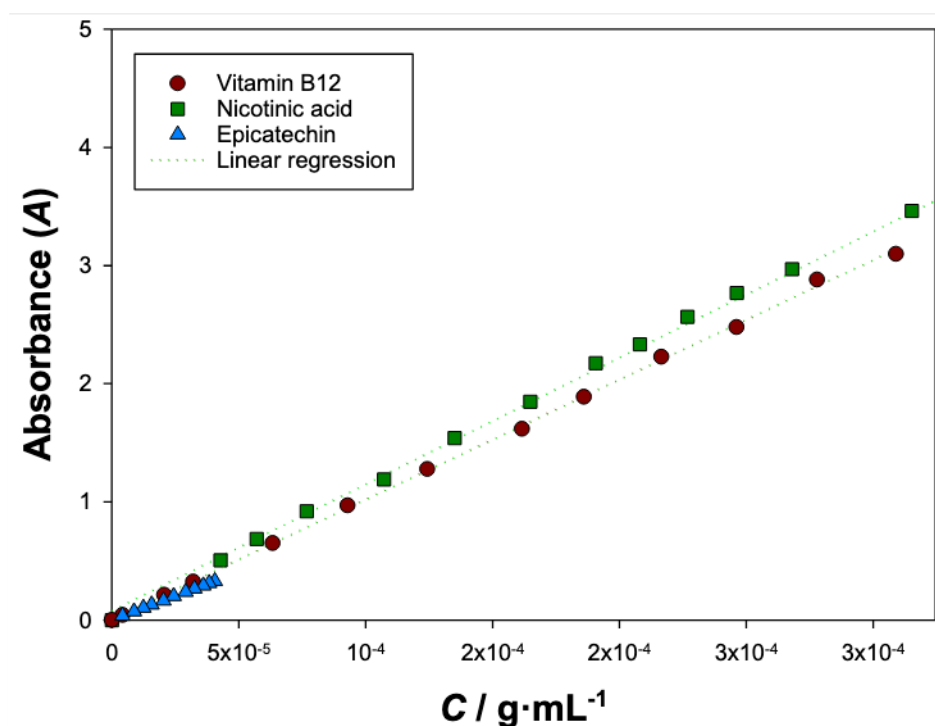


Figure 5. UV-Vis absorbance calibration curves at pH = 7.5 for epicatechin (278 nm), vitamin B12 (363 nm), and nicotinic acid (264 nm), with $T = 298.15 \text{ K}$ and $P = 0.1 \text{ MPa}$. The first-degree fittings follow equations: $A = 8091.2 \times C_E \text{ (g}\cdot\text{mL}^{-1}) + 0.0027$ with a determination coefficient (R^2) of 0.9998, $A = 10024 \times C_{B12} \text{ (g}\cdot\text{mL}^{-1}) + 0.0123$ with $R^2 = 0.9998$, and $A = 10630 \times C_{NA} \text{ (g}\cdot\text{mL}^{-1}) + 0.1000$ with $R^2 = 0.9993$, respectively.

3.3. Partitioning of Biomolecules

The applied ATPS were studied in previous works of the research group [24,25], so their liquid–liquid equilibria (LLE) were not determined in this work, and the partitioning of biomolecules was conducted at 298.15 K and 0.1 MPa in the previously reported tie-lines, which can be observed in Table 3.

Table 3. Determined tie-lines for the ATPS {ethyl lactate (1) + organic salt (2) + water (3)} used in this work at 298.15 K and 0.1 MPa ^{a,b} [24,25].

Tie Line	Feed		Phase	Separation		
	$w_1/m\%$	$w_2/m\%$		$w_1/m\%$	$w_2/m\%$	pH
{ethyl lactate (1) + disodium tartrate (2) + water (3)} [25]						
1	28.0	12.5	Top	51.4	3.7	6.18
			Bottom	15.5	17.0	6.10
2	30.0	13.0	Top	57.5	2.7	6.13
			Bottom	11.6	19.8	6.17
3	32.5	13.3	Top	63.1	2.0	6.13
			Bottom	9.0	22.3	6.18
4	35.5	13.8	Top	68.9	1.5	6.15
			Bottom	7.0	24.8	6.18
5	38.0	14.0	Top	72.4	1.3	6.11
			Bottom	6.0	26.2	6.17
{ethyl lactate (1) + trisodium citrate (2) + water (3)} [24]						
1	30.0	11.0	Top	51.7	3.0	7.00
			Bottom	16.0	15.7	6.98
2	32.0	11.4	Top	57.5	2.0	6.98
			Bottom	12.3	18.5	6.96
3	34.3	11.7	Top	61.5	1.4	6.98
			Bottom	9.8	20.7	6.97
4	36.5	12.1	Top	65.0	1.0	7.00
			Bottom	7.9	23.0	7.00
5	38.5	12.3	Top	67.7	0.7	6.98
			Bottom	6.8	24.7	6.97
6	40.6	12.6	Top	70.1	0.5	6.98
			Bottom	5.5	26.6	7.00
{ethyl lactate (1) + tripotassium citrate (2) + water (3)} [24]						
1	35.5	12.6	Top	57.9	3.9	7.21
			Bottom	15.0	20.3	7.39
2	37.5	13.0	Top	61.7	3.4	7.22
			Bottom	11.5	23.2	7.41
3	39.2	13.5	Top	67.4	2.1	7.19
			Bottom	9.1	25.8	7.37
4	41.1	13.9	Top	70.4	1.6	7.23
			Bottom	7.5	28.2	7.41
5	43.0	14.3	Top	73.6	1.1	7.12
			Bottom	6.0	31.0	7.39
6	44.6	14.8	Top	75.8	0.9	7.22
			Bottom	5.2	33.1	7.43

^a w_i stands for the mass percentage ($m\%$) of species i ; ^b standard uncertainties (u) are: $u(T) = 0.2$ K, $u(P) = 10$ kPa, $u(w_i) = 10^{-1}$, and $u(\text{pH}) = 10^{-2}$ [24,25].

So as to quantify the partition of the studied biomolecules, after phase equilibrium was reached, the liquid phases were separated and mass (m), absorbance (A), pH, and density (ρ) were measured. Then, the mass losses (L_m) were calculated, in percentage, using Equation (4). The results are shown in Table 4.

$$L_m/\% = \frac{m_2}{m_1} \times 100 \quad (4)$$

Here, m_1 is the total mass (feed), and m_2 is the sum of masses of the two phases separated after equilibrium was reached.

Table 4. Experimental mass (m), UV-Vis absorbance () at chosen wavelength (), density (ρ), pH, and mass loss (L_m) for the top and bottom phases in the extraction of epicatechin, cyanocobalamin, and nicotinic acid using the ATPS {ethyl lactate (1) + Na₂Tartrate or Na₃Citrate or K₃Citrate (2) + water (3)} at 298.15 K and 0.1 MPa ^a.

Tie Line	Phase	m/g	$L_m/\%$	$\rho/g \cdot mL^{-1}$		pH
Epicatechin = 278 nm)–Na₂Tartrate						
1	Top	3.6786	0.48	0.8346	1.05790	6.880
	Bottom	6.4186		0.4077	1.12550	6.862
2	Top	4.4509	0.10	0.8870	1.04840	6.996
	Bottom	5.5871		0.3671	1.13730	6.873
3	Top	4.3920	1.95	0.9332	1.04750	7.014
	Bottom	5.4675		0.3379	1.15600	6.896
4	Top	4.6811	0.74	0.9686	1.04550	7.049
	Bottom	5.3176		0.3339	1.17670	7.078
5	Top	5.1993	1.92	0.9896	1.04210	7.083
	Bottom	4.6718		0.3297	1.19110	6.986
Epicatechin = 278 nm)–K₃Citrate						
1	Top	4.4828	0.19	0.8568	1.05867	8.215
	Bottom	5.5222		0.2778	1.14870	8.248
2	Top	4.8564	1.41	0.8888	1.05425	8.285
	Bottom	5.0553		0.2320	1.16630	8.283
3	Top	5.1306	1.44	0.9502	1.05210	8.244
	Bottom	4.8115		0.2056	1.17672	8.321
4	Top	5.2578	0.85	0.9688	1.04671	8.266
	Bottom	4.8111		0.1992	1.19459	8.485
5	Top	5.4584	1.17	0.9984	1.04583	8.291
	Bottom	4.5713		0.1882	1.21058	8.509
6	Top	5.7649	1.65	1.0392	1.04572	8.344
	Bottom	4.3962		0.1811	1.21871	8.515
Vitamin B12 (= 363 nm)–Na₂Tartrate						
1	Top	3.3444	1.39	2.0127	1.05920	6.990
	Bottom	6.6009		1.1287	1.12560	6.905
2	Top	3.8218	1.39	2.2431	1.06760	7.010
	Bottom	6.0977		0.8812	1.10820	6.958
3	Top	4.5850	1.36	2.3748	1.05170	6.952
	Bottom	5.3460		0.5605	1.12960	7.063
4	Top	5.1427	0.49	2.3930	1.04900	6.965
	Bottom	4.8684		0.3193	1.14630	7.063
5	Top	5.4989	0.48	2.3171	1.04580	6.988
	Bottom	4.5034		0.2393	1.16320	7.150
Vitamin B12 (= 363 nm)–K₃Citrate						
1	Top	4.6756	1.29	2.3753	1.05970	8.103
	Bottom	5.2595		0.5091	1.15070	8.068
2	Top	5.0931	0.91	2.3588	1.05330	8.141
	Bottom	4.8615		0.3312	1.16280	8.097
3	Top	5.1493	0.88	2.4601	1.05020	8.188
	Bottom	4.8149		0.2024	1.17200	8.108
4	Top	5.2956	1.17	2.4048	1.04800	8.206
	Bottom	4.6424		0.1611	1.19390	8.156
5	Top	5.418	0.97	2.4107	1.04550	8.233
	Bottom	4.5434		0.1183	1.20940	8.191
6	Top	5.5163	1.15	2.3630	1.04470	8.281
	Bottom	4.4272		0.0965	1.21970	8.263

Table 4. Cont.

Tie Line	Phase	<i>m</i> /g	<i>L_m</i> /%	<i>ρ</i> /g·mL ⁻¹		pH
Nicotinic acid (= 264 nm)–Na ₂ Tartrate						
1	Top	3.0821	1.03	4.0890	1.05322	6.619
	Bottom	6.8828		2.7974	1.12553	6.531
2	Top	3.4818	0.64	4.3159	1.05680	6.629
	Bottom	6.6076		2.5573	1.12730	6.529
3	Top	3.9679	1.31	4.5031	1.05280	6.638
	Bottom	5.9567		2.3235	1.13440	6.496
4	Top	4.5769	1.24	4.6137	1.04670	6.568
	Bottom	5.3389		2.0370	1.15830	6.539
5	Top	5.0313	1.09	4.6525	1.04640	6.644
	Bottom	4.9116		1.8679	1.17280	6.618
Nicotinic acid (= 264 nm)–Na ₃ Citrate						
1	Top	3.6279	0.76	4.0313	1.05381	7.644
	Bottom	6.4795		2.3153	1.12229	7.534
2	Top	4.0828	0.21	4.3514	1.04788	7.748
	Bottom	5.8773		2.0339	1.13681	7.554
3	Top	4.5328	0.21	4.3578	1.04558	7.685
	Bottom	5.4912		1.8313	1.15010	7.551
4	Top	4.7552	0.48	4.3915	1.04354	7.735
	Bottom	5.2350		1.6074	1.16720	7.603
5	Top	4.9717	0.76	4.4329	1.04209	7.721
	Bottom	4.9846		1.4982	1.18528	7.621
6	Top	5.1887	0.42	4.1538	1.04118	7.851
	Bottom	4.8186		1.3575	1.19160	8.048

^a The measurement uncertainties u are: $u(m) = 10^{-4}$ g, $u(L_m) = 10^{-4}$, $u(\rho) = 3 \times 10^{-5}$ g·mL⁻¹ and $u(\text{pH}) = 10^{-3}$.

As seen in Table 4, UV-Vis absorbances were always higher for top phases, so all the studied biomolecules preferentially diffused into the ethyl-lactate-rich phase. Generally, the measured pH and density values of the phases were larger for the ATPS containing tripotassium citrate and smaller for the ATPS based on disodium tartrate. Moreover, pH values for the phases of each tie line in each system were alike, which implies similar distribution of electrical charges and, consequently, similar mean electrical charge (q) in both phases of the same tie-line composition. This way, the phases presented homogeneous characteristics and a single calibration curve could be applied.

Since using different tie-line compositions caused different pH values in the liquid phases (as seen in Table 4), it was necessary to understand if the distribution of biomolecule stages was similar between phases of different tie-line composition (for the same system). As Figure 6 shows, the ATPS {ethyl lactate (1) + disodium tartrate (2) + water (3)} ensured similar and well-defined stages for all the biomolecules, so its tie-line compositions yielded a homogenous biomolecule extract. The same conclusion can be drawn from {ethyl lactate (1) + trisodium citrate (2) + water (3)} in extracting nicotinic acid and from {ethyl lactate (1) + tripotassium citrate (2) + water (3)} in extracting cyanocobalamin, as Figures S6 and S7 in the Supplementary Materials, respectively, show. However, as can be seen in Figure S7 in the Supplementary Materials, the different tie-line compositions of {ethyl lactate (1) + tripotassium citrate (2) + water (3)} caused different distributions of biomolecule stages between the tie lines for epicatechin, particularly to what concerns the neutral and mono negatively charged species, originating more heterogeneous extracts.

With the measured UV-Vis absorbances and with the determined calibration curves (Figure 5), after subtracting the blanks, the concentrations of each biomolecule in each ATPS were determined, and a partition coefficient (K) was determined for each tie-line composition using Equation (5). These results can be observed in Table 5.

$$K_i = \frac{C_i^{\text{top}}}{C_i^{\text{bottom}}} \quad (5)$$

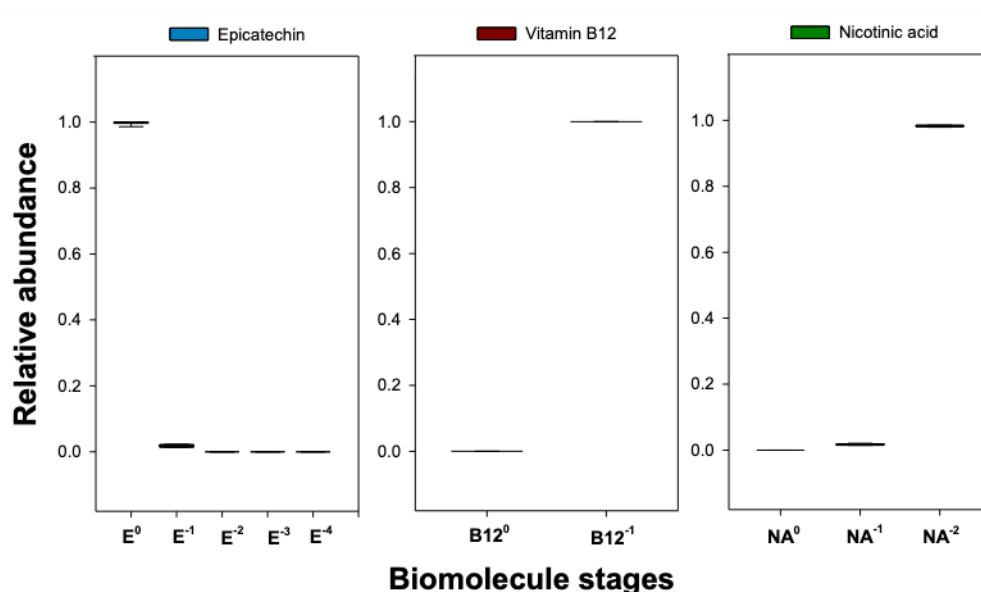


Figure 6. Influence of the tie-line compositions in the fraction of the biomolecule stages of epicatechin, cyanocobalamin, and nicotinic acid in the ATPS {ethyl lactate (1) + disodium tartrate (2) + water (3)} at 298.15 K and 0.1 MPa. E^0 , E^{-1} , E^{-2} , E^{-3} , and E^{-4} stand for the biomolecule stages of epicatechin with electrical charges equal to 0, -1 , -2 , -3 , and -4 e, respectively; $B12^0$ and $B12^{-1}$ stand for the biomolecule stages of cyanocobalamin with electrical charges equal to 0 and -1 e, respectively; NA^0 , NA^{-1} , and NA^{-2} stand for the biomolecule stages of nicotinic acid with electrical charges equal to 0, -1 , and -2 e, respectively, and e stands for the elementary charge (1.602×10^{-19} C).

Table 5. Calculated concentration of biomolecule (C) for each phase, partition coefficients (K) for each tie-line composition, and tie-line lengths (TLL) for the extraction of epicatechin, cyanocobalamin, and nicotinic acid using the ATPS {ethyl lactate (1) + Na_2 Tartrate or Na_3 Citrate or K_3 Citrate (2) + water (3)} at 298.15 K and 0.1 MPa.

Tie Line	Phase	C/g·mL ¹	K	TLL/% [24,25]
Epicatechin–Na ₂ Tartrate				
1	Top	2.75 × 10 ⁵	2.12	38.33
	Bottom	1.30 × 10 ⁵		
2	Top	2.70 × 10 ⁵	2.56	49.02
	Bottom	1.06 × 10 ⁵		
3	Top	3.00 × 10 ⁵	3.71	57.82
	Bottom	8.09 × 10 ⁶		
4	Top	3.04 × 10 ⁵	4.10	66.14
	Bottom	7.43 × 10 ⁶		
5	Top	2.87 × 10 ⁵	5.43	70.90
	Bottom	5.29 × 10 ⁶		
Epicatechin–K ₃ Citrate				
1	Top	3.20 × 10 ⁵	4.75	45.91
	Bottom	6.73 × 10 ⁶		
2	Top	3.21 × 10 ⁵	6.97	54.02
	Bottom	4.60 × 10 ⁶		
3	Top	3.26 × 10 ⁵	12.28	62.96
	Bottom	2.65 × 10 ⁶		
4	Top	3.23 × 10 ⁵	16.09	68.28
	Bottom	2.01 × 10 ⁶		
5	Top	3.14 × 10 ⁵	21.43	73.92
	Bottom	1.47 × 10 ⁶		
6	Top	3.04 × 10 ⁵	24.86	77.66
	Bottom	1.22 × 10 ⁶		

Table 5. Cont.

Tie Line	Phase	C/g·mL ¹	K	TLL/% [24,25]
Vitamin B12–Na ₂ Tartrate				
1	Top	6.15×10^{-4}	1.87	38.33
	Bottom	6.11×10^{-4}		
2	Top	7.79×10^{-4}	2.74	49.02
	Bottom	4.38×10^{-4}		
3	Top	1.01×10^{-3}	4.91	57.82
	Bottom	2.22×10^{-4}		
4	Top	1.14×10^{-3}	10.35	66.14
	Bottom	9.53×10^{-5}		
5	Top	1.18×10^{-3}	15.96	70.90
	Bottom	5.44×10^{-5}		
Vitamin B12–K ₃ Citrate				
1	Top	2.31×10^{-4}	5.26	45.91
	Bottom	4.39×10^{-5}		
2	Top	2.30×10^{-4}	8.80	54.02
	Bottom	2.61×10^{-5}		
3	Top	2.40×10^{-4}	17.33	62.96
	Bottom	1.38×10^{-5}		
4	Top	2.34×10^{-4}	24.88	68.28
	Bottom	9.40×10^{-6}		
5	Top	2.34×10^{-4}	46.05	73.92
	Bottom	5.09×10^{-6}		
6	Top	2.30×10^{-4}	78.56	77.66
	Bottom	2.92×10^{-6}		
Nicotinic acid–Na ₂ Tartrate				
1	Top	3.15×10^{-4}	1.41	38.33
	Bottom	2.24×10^{-4}		
2	Top	3.30×10^{-4}	1.66	49.02
	Bottom	1.99×10^{-4}		
3	Top	3.45×10^{-4}	1.91	57.82
	Bottom	1.81×10^{-4}		
4	Top	3.52×10^{-4}	2.30	66.14
	Bottom	1.53×10^{-4}		
5	Top	3.51×10^{-4}	2.60	70.90
	Bottom	1.35×10^{-4}		
Nicotinic acid–Na ₃ Citrate				
1	Top	3.23×10^{-4}	1.67	37.85
	Bottom	1.94×10^{-4}		
2	Top	3.47×10^{-4}	2.04	48.18
	Bottom	1.70×10^{-4}		
3	Top	3.46×10^{-4}	2.28	55.17
	Bottom	1.52×10^{-4}		
4	Top	3.46×10^{-4}	2.62	61.17
	Bottom	1.32×10^{-4}		
5	Top	3.48×10^{-4}	2.86	65.44
	Bottom	1.22×10^{-4}		
6	Top	3.67×10^{-4}	3.55	69.68
	Bottom	1.03×10^{-4}		

Here, i is the tie-line number, and C_i^{top} and C_i^{bottom} correspond to the biomolecule's concentration in the top and bottom phases, respectively.

As can be observed in Table 5, the extraction of vitamin B12 in the ATPS {ethyl lactate (1) + K₃Citrate (2) + water (3)} presented the largest partition coefficients, reaching $K = 78.56$ with TLL = 77.66%. Conversely, nicotinic acid in {ethyl lactate (1) + Na₂Tartrate (2) + water (3)} yielded the worst results, obtaining $K = 2.60$ for the longest tie line (TLL = 70.90%). Moreover, all the systems achieved partition coefficients above unity, which means that the

top phases' concentrations of biomolecule were always larger than the ones of the bottom phases. Therefore, ethyl lactate, which is mostly present in the top phases, was successful in extracting the biomolecules.

Furthermore, as Figure 7 shows, all biomolecules suffered an increase in the top phase concentration for longer tie lines, *i.e.*, for more distinct top and bottom compositions, so ethyl lactate presents good affinity for these species. The more positive the slope of the lines, the more favoured solute migration for the top phase is with growing tie-line length, so ethyl lactate presents more affinity for cyanocobalamin. Generally, a close to linear behaviour was verified for the natural logarithm of the partition coefficients ($\ln K$) with the tie-line lengths (TLL).

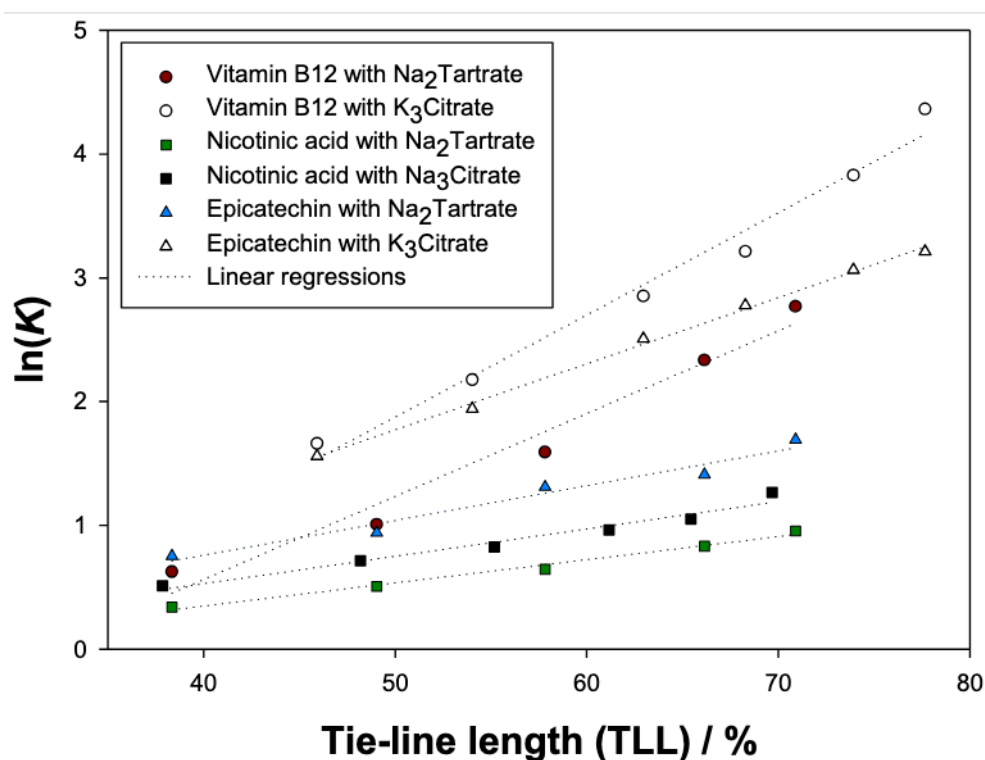


Figure 7. Relation of the tie-line length (TLL) [24,25] with the natural logarithm of the experimental partition coefficients (K) in the ATPS {ethyl lactate (1) + $\text{Na}_2\text{Tartrate}$ or $\text{Na}_3\text{Citrate}$ or $\text{K}_3\text{Citrate}$ (2) + water (3)} at 298.15 K and 0.1 MPa for epicatechin, vitamin B12, and nicotinic acid.

3.4. Mass Balance

To ensure the validity of the reported partition coefficients of Table 5, it is of the utmost importance to validate the analytical method by performing a mass balance on the biomolecules under study, *i.e.*, verifying that all the biomolecule mass is being considered. First, the liquid volumes (V) of all the phases (top and bottom) were determined using:

$$V_j = \frac{m_j}{\rho_j} \quad (6)$$

where V_j is the liquid phase volume, m_j is the measured mass, and ρ_j is the measured density for phase j .

Then, the mass balance was checked by calculating the solute losses (L_s) using:

$$L_s/\% = \frac{m_{s2}}{m_{s1}} \times 100 \quad (7)$$

where m_{s1} is the added mass of biomolecule (present in 1 mL of stock solution), and m_{s2} is the total quantified mass of biomolecule, which was calculated using:

$$m_{s2} = V_i^{\text{top}} C_i^{\text{top}} + V_i^{\text{bottom}} C_i^{\text{bottom}} \quad (8)$$

where V_i^{top} and V_i^{bottom} are the calculated experimental volumes of the top and bottom phases, respectively, and i refers to the tie-line number.

Further, the extraction efficiencies of each tie line (E) were determined with:

$$E/\% = \frac{m_{\text{top}}}{m_{s1}} \times 100 \quad (9)$$

where m_{top} is the quantified mass of biomolecule in the top phase.

Since the solute losses quantified using Equation (7) may be in the top phase, an extraction efficiency interval can be found using the values determined for E as the minimum boundary and summing the absolute value of L_s with E for the maximum limit. All these results are presented in Table 6.

Table 6. Calculated solute losses (L_s), extraction efficiency (E) intervals, and tie-line lengths (TLL) for the extraction of epicatechin, cyanocobalamin, and nicotinic acid in the ATPS {ethyl lactate (1) + Na₂Tartrate or Na₃Citrate or K₃Citrate (2) + water (3)} at 298.15 K and 0.1 MPa.

Tie line	$L_s/\%$	$E/\%$	TLL/% [24,25]
Epicatechin—Na₂ Tartrate			
1	1.12	55.7–56.9	38.33
2	2.37	67.2–69.6	49.02
3	4.11	73.5–77.6	57.82
4	1.21	79.2–80.4	66.14
5	4.41	83.4–87.8	70.90
Epicatechin—K₃ Citrate			
1	1.69	79.4–81.1	45.91
2	2.04	86.3–88.4	54.02
3	1.83	91.9–93.7	62.96
4	1.55	93.8–95.3	68.28
5	1.20	95.6–96.8	73.92
6	0.40	97.0–97.5	77.66
Vitamin B12—Na₂ Tartrate			
1	1.86	49.2–51.1	38.33
2	2.48	62.5–64.9	49.02
3	2.08	80.2–82.3	57.82
4	1.37	91.0–92.4	66.14
5	0.88	94.8–95.6	70.90
Vitamin B12—K₃ Citrate			
1	2.37	81.6–84.0	45.91
2	1.61	89.6–91.2	54.02
3	1.33	94.1–95.5	62.96
4	2.39	94.7–97.1	68.28
5	1.31	97.2–98.5	73.92
6	1.68	97.5–99.2	77.66
Nicotinic acid—Na₂ Tartrate			
1	0.91	39.9–40.8	38.33
2	2.36	47.1–49.5	49.02
3	2.71	56.2–59.0	57.82
4	2.93	66.6–69.5	66.14
5	2.92	72.7–75.7	70.90

Table 6. Cont.

Tie line	$L_s/\%$	$E/\%$	TLL/% [24,25]
Nicotinic acid–Na₃Citrate			
1	2.32	48.7–51.0	37.85
2	2.38	59.2–61.6	48.18
3	2.49	65.8–68.3	55.17
4	4.94	69.1–74.0	61.17
5	4.76	72.8–77.6	65.44
6	1.60	80.1–81.7	69.68

As Table 6 shows, low solute losses were obtained for epicatechin (<5%), vitamin B12 (<3%), and nicotinic acid (<5%). Therefore, the validity of the analytical method was assured, confirming the reported partition coefficients (K) and extraction efficiencies (E). Moreover, vitamin B12 presented the largest extraction efficiencies, and E increased with growing tie-line length (TLL) for all the studied biomolecules. In Figure 8, the extraction efficiencies (E) were plotted in the function of the tie-line lengths (TLL) to ease comparison.

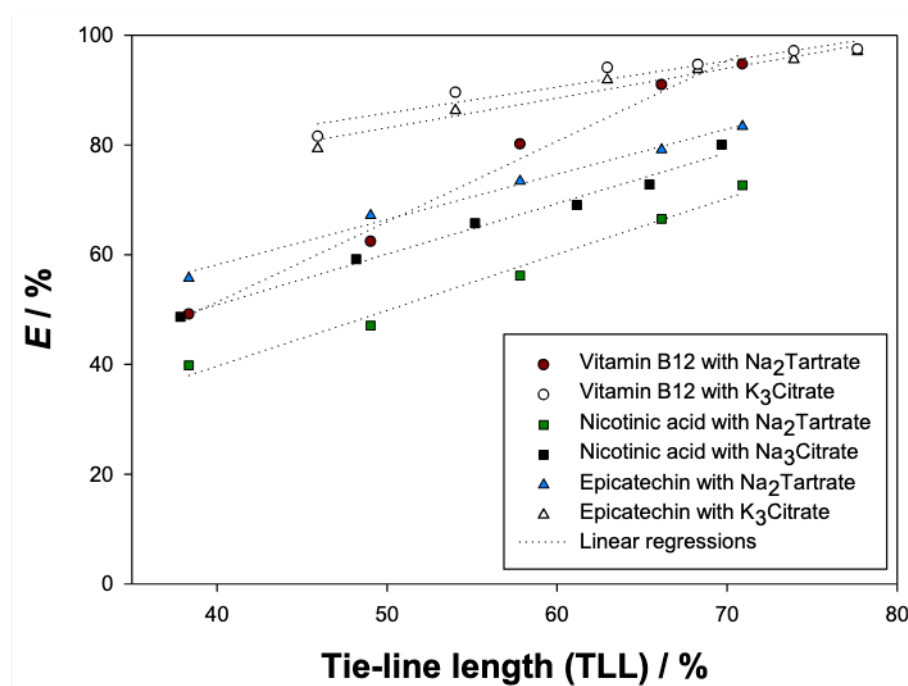


Figure 8. Relation of the tie-line length (TLL) [24,25] with the extraction efficiencies (E) in the ATPS {ethyl lactate (1) + Na₂Tartrate or Na₃Citrate or K₃Citrate (2) + water (3)} at 298.15 K and 0.1 MPa for epicatechin, cyanocobalamin, and nicotinic acid.

As seen in Figure 8, the longest tie-lines provided the highest extraction efficiencies (E). Therefore, solute migration to the top phases was favoured by more distinct compositions of the phases, *i.e.*, higher concentration of ethyl lactate in the top phases and higher salt concentration in the bottom phases. Epicatechin and vitamin B12 reached extraction efficiencies close to 100%, while nicotinic acid achieved, at maximum, 81.7%.

By observing Figures 7 and 8, it can be concluded that the best system for the extraction of vitamin B12 (cyanocobalamin) at 298.15 K and 0.1 MPa is {ethyl lactate (1) + K₃Citrate (2) + water (3)}, since it yields larger partition coefficients (presents a more top phase-centred solute distribution) and larger extraction efficiencies (top phases retain a more significant fraction of the added biomolecule) than {ethyl lactate (1) + Na₂Tartrate (2) + water (3)}. Following the same logic, {ethyl lactate (1) + K₃Citrate (2) + water (3)} is better than {ethyl lactate (1) + Na₂Tartrate (2) + water (3)} at extracting epicatechin, and {ethyl lactate (1) + Na₃Citrate (2) + water (3)} provides more reliable extractive media for nicotinic acid than

{ethyl lactate (1) + Na₂Tartrate (2) + water (3)}. These findings follow the generally observed trend that citrate-based organic salts ensure more efficient extractions of biomolecules than tartrate-based organic salts.

4. Conclusions

Reducing food waste and converting it to societal benefits has become a topic of great importance due to the exponential growth of the human population and the inefficient use of natural resources. Biomolecules such as polyphenols (*e.g.*, epicatechin) and vitamins (*e.g.*, cyanocobalamin and nicotinic acid) are present in some vegetables, fruits, and legumes, for which their presence in food waste is inevitable. These chemical species conceal unique nutritive and medicinal properties, so they have been added to pharmaceuticals (*e.g.*, food supplements) and cosmetics (*e.g.*, creams and shampoos).

In this work, partition studies of epicatechin, vitamin B12 (cyanocobalamin), and nicotinic acid were successfully conducted in the ATPS {ethyl lactate (1) + Na₂Tartrate or Na₃Citrate or K₃Citrate (2) + water (3)} at 298.15 K and 0.1 MPa for future valorisation of food wastes such as vegetable peels and fruit pomaces. The largest partition coefficients (*K*) and extraction efficiencies (*E*) were obtained for vitamin B12 (*K* = 78.56, *E* = 97.5%) and for epicatechin (*K* = 24.86, *E* = 97.0%) for the longest tie line TLL = 77.66% in the ATPS {ethyl lactate (1) + tripotassium citrate (2) + water (3)}. Therefore, this is the most efficient extractive system for future valorisation of vitamin-B12-rich (*e.g.*, potato peels) and epicatechin-rich (*e.g.*, apple peels) food waste.

All the applied ATPS provided partition coefficients larger than unity, for which they were considered successful in the extraction of the studied biomolecules. The reported extraction efficiencies (*E*) and partition coefficients (*K*) were validated by the verified low biomolecule mass losses in quantification for vitamin B12 (<3%), epicatechin (<5%), and nicotinic acid (<5%), which were achieved after a thorough study of the influence of pH in the UV–Vis absorbance spectra of these biomolecules.

Supplementary Materials: The following supporting information can be downloaded at <https://www.mdpi.com/article/10.3390/molecules27227838/s1>: Figure S1: Influence of pH in the UV-Vis absorbance spectra of vitamin B12 at 298.15 K and 0.1 MPa; Figure S2: Influence of pH in the UV-Vis absorbance spectra of nicotinic acid at 298.15 K and 0.1 MPa; Figure S3: UV-Vis absorbance spectra of the aqueous stock solution of epicatechin in the moment of preparation and after 3 days of settling at 298.15 K and 0.1 MPa; Figure S4: UV-Vis absorbance spectra of the aqueous stock solution of vitamin B12 in the moment of preparation and after 3 days of settling at 298.15 K and 0.1 MPa; Figure S5: UV-Vis absorbance spectra of the aqueous stock solution of nicotinic acid in the moment of preparation and after 3 days of settling at 298.15 K and 0.1 MPa; Figure S6: Influence of the tie-line compositions in the fraction of the biomolecule stages of nicotinic acid in the ATPS {ethyl lactate (1) + trisodium citrate (2) + water (3)} at 298.15 K and 0.1 MPa; Figure S7: Influence of the tie-line compositions in the fraction of the biomolecule stages of epicatechin and cyanocobalamin (vitamin B12) in the ATPS {ethyl lactate (1) + tripotassium citrate (2) + water (3)} at 298.15 K and 0.1 MPa; Table S1: Calculated fractions of each biomolecule stage and mean electrical charge (*q*) at different pH values for epicatechin; Table S2: Calculated fractions of each biomolecule stage and mean electrical charge (*q*) at different pH values for vitamin B12; Table S3: Calculated fractions of each biomolecule stage and mean electrical charge (*q*) at different pH values for nicotinic acid.

Author Contributions: Conceptualization, P.V. and E.A.M.; methodology, P.V.; validation, P.V., L.M. and E.A.M.; formal analysis, P.V.; investigation, P.V. and L.M.; writing—original draft preparation, P.V. and L.M.; writing—review and editing, P.V.; visualization, P.V. and E.A.M.; supervision, E.A.M.; funding acquisition, P.V. and E.A.M. All authors have read and agreed to the published version of the manuscript.

Funding: This research was funded by ALiCE [LA/P/0045/2020] and LSRE-LCM [UIDB/50020/2020 and UIDP/50020/2020] and funded by national funds through FCT/MCTES (PIDDAC). Pedro Velho (2021.06626.BD) and Luís Marques (VERAO_COM_CIENCIA_2022_LSRE-LCM) are grateful for the funding support from FCT.

Institutional Review Board Statement: Not applicable.

Informed Consent Statement: Not applicable.

Data availability Statement: The data presented in this study are available on request from the corresponding author.

acknowledgments: This work was supported by ALiCE (LA/P/0045/2020) and LSRE-LCM (UIDB/50020/2020 and UIDP/50020/2020) and funded by national funds through FCT/MCTES (PID-DAC). Pedro Velho (2021.06626.BD) and Luís Marques (VERAO_COM_CIENCIA_2022_LSRE-LCM) are grateful for the funding support from FCT.

Conflicts of Interest: The authors declare no conflict of interest.

References

1. Eičaitė, O.; Baležentis, T.; Ribašauskienė, E.; Morkūnas, M.; Melnikienė, R.; Štreimikienė, D. Food waste in the retail sector: A survey-based evidence from Central and Eastern Europe. *J. Retail. Consum. Serv.* **2022**, *69*, 103116. [\[CrossRef\]](#)
2. Ananda, J.; Karunasena, G.G.; Pearson, D. Identifying interventions to reduce household food waste based on food categories. *Food Policy* **2022**, *111*, 102324. [\[CrossRef\]](#)
3. Siddiqui, Z.; Hagare, D.; Jayasena, V.; Swick, R.; Rahman, M.M.; Boyle, N.; Ghodrati, M. Recycling of food waste to produce chicken feed and liquid fertiliser. *Waste Manag.* **2021**, *131*, 386–393. [\[CrossRef\]](#) [\[PubMed\]](#)
4. Ojha, S.; Bußler, S.; Schlüter, O.K. Food waste valorisation and circular economy concepts in insect production and processing. *Waste Manag.* **2020**, *118*, 600–609. [\[CrossRef\]](#) [\[PubMed\]](#)
5. Caldeira, C.; Vlysidis, A.; Fiore, G.; De Laurentiis, V.; Vignali, G.; Sala, S. Sustainability of food waste biorefinery: A review on valorisation pathways, techno-economic constraints, and environmental assessment. *Bioresour. Technol.* **2020**, *312*, 123575. [\[CrossRef\]](#)
6. Tournour, H.H.; Segundo, M.A.; Magalhães, L.M.; Barreiros, L.; Queiroz, J.; Cunha, L. Valorization of grape pomace: Extraction of bioactive phenolics with antioxidant properties. *Ind. Crop. Prod.* **2015**, *74*, 397–406. [\[CrossRef\]](#)
7. Ferreira, S.M.; Santos, L. From by-product to functional ingredient: Incorporation of avocado peel extract as an antioxidant and antibacterial agent. *Innov. Food Sci. Emerg. Technol.* **2022**, *80*, 103116. [\[CrossRef\]](#)
8. Tavares, L.; Smaoui, S.; Lima, P.S.; de Oliveira, M.M.; Santos, L. Propolis: Encapsulation and application in the food and pharma-ceutical industries. *Trends Food Sci. Technol.* **2022**, *127*, 169–180. [\[CrossRef\]](#)
9. Hatti-Kaul, R. Aqueous Two-Phase Systems: A General Overview. *Mol. Biotechnol.* **2001**, *19*, 269–278. [\[CrossRef\]](#)
10. Saha, N.; Sarkar, B.; Sen, K. Aqueous biphasic systems: A robust platform for green extraction of biomolecules. *J. Mol. Liq.* **2022**, *363*, 119882. [\[CrossRef\]](#)
11. Wysoczanska, K.; Macedo, E.A. Influence of the Molecular Weight of PEG on the Polymer/Salt Phase Diagrams of Aqueous Two-Phase Systems. *J. Chem. Eng. Data* **2016**, *61*, 4229–4235. [\[CrossRef\]](#)
12. Wysoczanska, K.; Do, H.T.; Held, C.; Sadowski, G.; Macedo, E.A. Effect of different organic salts on amino acids partition behaviour in PEG-salt ATPS. *Fluid Phase Equilibria* **2018**, *456*, 84–91. [\[CrossRef\]](#)
13. Gomes, G.A.; Azevedo, A.M.; Aires-Barros, M.R.; Prazeres, D.M.F. Purification of plasmid DNA with aqueous two phase systems of PEG 600 and sodium citrate/ammonium sulfate. *Sep. Purif. Technol.* **2009**, *65*, 22–30. [\[CrossRef\]](#)
14. Panas, P.; Lopes, C.; Cerri, M.O.; Ventura, S.P.; Santos-Ebinuma, V.C.; Pereira, J.F. Purification of clavulanic acid produced by *Streptomyces clavuligerus* via submerged fermentation using polyethylene glycol/cholinium chloride aqueous two-phase systems. *Fluid Phase Equilibria* **2017**, *450*, 42–50. [\[CrossRef\]](#)
15. Liu, C.; Liu, S.; Zhang, L.; Wang, X.; Ma, L. Partition Behavior in Aqueous Two-Phase System and Antioxidant Activity of Flavonoids from *Ginkgo biloba*. *Appl. Sci.* **2018**, *8*, 2058. [\[CrossRef\]](#)
16. Nascimento, K.S.; Rosa, P.; Cavada, B.; Azevedo, A.M.; Aires-Barros, M.R. Partitioning and recovery of Canavalia brasiliensis lectin by aqueous two-phase systems using design of experiments methodology. *Sep. Purif. Technol.* **2010**, *75*, 48–54. [\[CrossRef\]](#)
17. Dolzhenko, A.V. Ethyl lactate and its aqueous solutions as sustainable media for organic synthesis. *Sustain. Chem. Pharm.* **2020**, *18*, 100322. [\[CrossRef\]](#)
18. Dandia, A.; Jain, A.K.; Laxkar, A.K. Ethyl lactate as a promising bio based green solvent for the synthesis of spiro-oxindole derivatives via 1,3-dipolar cycloaddition reaction. *Tetrahedron Lett.* **2013**, *54*, 3929–3932. [\[CrossRef\]](#)
19. Pereira, C.; Silva, V.M.T.M.; Rodrigues, A.E. Fixed Bed Adsorptive Reactor for Ethyl Lactate Synthesis: Experiments, Modelling, and Simulation. *Sep. Sci. Technol.* **2009**, *44*, 2721–2749. [\[CrossRef\]](#)
20. Pereira, C.; Zabka, M.; Silva, V.M.; Rodrigues, A.E. A novel process for the ethyl lactate synthesis in a simulated moving bed reactor (SMBR). *Chem. Eng. Sci.* **2009**, *64*, 3301–3310. [\[CrossRef\]](#)
21. Velho, P.; Oliveira, I.; Gómez, E.; Macedo, E.A. pH Study and Partition of Riboflavin in an Ethyl Lactate-Based Aqueous Two-Phase System with Sodium Citrate. *J. Chem. Eng. Data* **2022**, *67*, 1985–1993. [\[CrossRef\]](#)
22. Kua, Y.L.; Gan, S.; Morris, A.; Ng, H.K. Optimization of simultaneous carotenes and vitamin E (tocols) extraction from crude palm olein using response surface methodology. *Chem. Eng. Commun.* **2018**, *205*, 596–609. [\[CrossRef\]](#)

23. Ishida, B.K.; Chapman, M.H. Carotenoid Extraction from Plants Using a Novel, Environmentally Friendly Solvent. *J. agric. Food Chem.* **2009**, *57*, 1051–1059. [[CrossRef](#)]
24. Velho, P.; Requejo, P.F.; Gómez, E.; Macedo, E.A. Novel ethyl lactate based ATPS for the purification of rutin and quercetin. *Sep. Purif. Technol.* **2020**, *252*, 117447. [[CrossRef](#)]
25. Requejo, P.F.; Velho, P.; Gómez, E.; Macedo, E.A. Study of Liquid–Liquid Equilibrium of Aqueous Two-Phase Systems Based on Ethyl Lactate and Partitioning of Rutin and Quercetin. *Ind. Eng. Chem. Res.* **2020**, *59*, 21196–21204. [[CrossRef](#)]
26. Lores, M.; Pajaro, M.; Álvarez-Casas, M.; Domínguez, J.; García-Jares, C. Use of ethyl lactate to extract bioactive compounds from *Cytisus scoparius*: Comparison of pressurized liquid extraction and medium scale ambient temperature systems. *Talanta* **2015**, *140*, 134–142. [[CrossRef](#)]
27. Kamalanathan, I.; Canal, L.; Hegarty, J.; Najdanovic-Visak, V. Partitioning of amino acids in the novel biphasic systems based on environmentally friendly ethyl lactate. *Fluid Phase Equilibria* **2018**, *462*, 6–13. [[CrossRef](#)]
28. Datta, S.; Bals, B.; Lin, Y.J.; Negri, M.; Datta, R.; Pasieta, L.; Ahmad, S.F.; Moradia, A.A.; Dale, B.; Snyder, S.W. An attempt towards simultaneous biobased solvent based extraction of proteins and enzymatic saccharification of cellulosic materials from distiller's grains and solubles. *Bioresour. Technol.* **2010**, *101*, 5444–5448. [[CrossRef](#)]
29. Zakrzewska, M.E.; Nunes, A.V.; Barot, A.R.; Fernandez-Castané, A.; Visak, Z.P.; Kiatkittipong, W.; Najdanovic-Visak, V. Extraction of antibiotics using aqueous two-phase systems based on ethyl lactate and thiosulphate salts. *Fluid Phase Equilibria* **2021**, *539*, 113022. [[CrossRef](#)]
30. Velho, P.; Gómez, E.; Macedo, E.A. Calculating the closest approach parameter for ethyl lactate-based ATPS. *Fluid Phase Equilibria* **2022**, *556*, 113389. [[CrossRef](#)]
31. Wu, X.; Li, R.; Zhao, Y.; Liu, Y. Separation of polysaccharides from *Spirulina platensis* by HSCCC with ethanol-ammonium sulfate ATPS and their antioxidant activities. *Carbohydr. Polym.* **2017**, *173*, 465–472. [[CrossRef](#)] [[PubMed](#)]
32. Velho, P.; Requejo, P.F.; Gómez, E.; Macedo, E.A. Thermodynamic study of ATPS involving ethyl lactate and different inorganic salts. *Sep. Purif. Technol.* **2021**, *275*, 119155. [[CrossRef](#)]
33. Li, Z.; Feng, Y.; Liu, X.; Wang, H.; Pei, Y.; Gunaratne, H.Q.N.; Wang, J. Light-Triggered Switchable Ionic Liquid Aqueous Two-Phase Systems. *CS Sustain. Chem. Eng.* **2020**, *8*, 15327–15335. [[CrossRef](#)]
34. Requejo, P.F.; Gómez, E.; Macedo, E.A. Partitioning of DNP-Amino Acids in New Biodegradable Choline Amino Acid/Ionic Liquid-Based Aqueous Two-Phase Systems. *J. Chem. Eng. Data* **2019**, *64*, 4733–4740. [[CrossRef](#)]
35. Amid, M.; Manap, M.Y.; Hussin, M.; Mustafa, S. A Novel Aqueous Two Phase System Composed of Surfactant and Xylitol for the Purification of Lipase from Pumpkin (*Cucurbita moschata*) Seed and Recycling of Phase Components. *Molecules* **2015**, *20*, 11184–11201. [[CrossRef](#)]
36. Panche, A.N.; Diwan, A.D.; Chandra, S.R. Flavonoids: An overview. *J. Nutr. Sci.* **2016**, *5*, e47. [[CrossRef](#)] [[PubMed](#)]
37. Dias, T.; Silva, M.R.; Damiani, C.; da Silva, F.A. Quantification of Catechin and Epicatechin in Foods by Enzymatic-Spectrophotometric Method with Tyrosinase. *Food Anal. Methods* **2017**, *10*, 3914–3923. [[CrossRef](#)]
38. Tsanova-Savova, S.; Ribarova, F.; Geroval, M. (+)-Catechin and (–)-epicatechin in Bulgarian fruits. *J. Food Compos. Anal.* **2005**, *18*, 691–698. [[CrossRef](#)]
39. Jiménez, R.; Duarte, J.; Perez-Vizcaino, F. Epicatechin: Endothelial Function and Blood Pressure. *J. agric. Food Chem.* **2012**, *60*, 8823–8830. [[CrossRef](#)]
40. Haskell-Ramsay, C.F.; Schmitt, J.; Actis-Goretta, L. The Impact of Epicatechin on Human Cognition: The Role of Cerebral Blood Flow. *Nutrients* **2018**, *10*, 986. [[CrossRef](#)]
41. Banjari, I.; Hjartåker, A. Dietary sources of iron and vitamin B12: Is this the missing link in colorectal carcinogenesis? *Med. Hypotheses* **2018**, *116*, 105–110. [[CrossRef](#)]
42. Green, R.; Allen, L.H.; Bjørke-Monsen, A.-L.; Brito, A.; Guéant, J.-L.; Miller, J.W.; Molloy, A.M.; Nexø, E.; Stabler, S.; Toh, B.-H.; et al. Vitamin B12 deficiency. *Nat. Rev. Dis. Primers* **2017**, *3*, 17040. [[CrossRef](#)] [[PubMed](#)]
43. Bodor, E.T.; Offermanns, S. Nicotinic acid: An old drug with a promising future. *J. Cereb. Blood Flow Metab.* **2008**, *153*, S68–S75. [[CrossRef](#)] [[PubMed](#)]
44. At, J.; Yaman, M. Determination of Nicotinic Acid and Nicotinamide Forms of Vitamin B3 (Niacin) in Fruits and Vegetables by HPLC Using Postcolumn Derivatization System. *Pak. J. Nutr.* **2019**, *18*, 563–570. [[CrossRef](#)]
45. Kennedy, J.; Munro, M.; Powell, H.; Porter, L.; Foo, L. The protonation reactions of catechin, epicatechin and related compounds. *Aust. J. Chem.* **1984**, *37*, 885–892. [[CrossRef](#)]
46. Brodie, J.D.; Poe, M. Proton magnetic resonance of vitamin B12 derivatives. Functioning of B12 coenzymes. *Biochemistry* **1972**, *11*, 2534–2542. [[CrossRef](#)] [[PubMed](#)]
47. Evans, R.F.; Herington, E.F.G.; Kynaston, W. Determination of dissociation constants of the pyridine-monocarboxylic acids by ultra-violet photoelectric spectrophotometry. *Trans. Faraday Soc.* **1953**, *49*, 1284–1292. [[CrossRef](#)]